Pharmacological Reports (2020) 72:1370–1382
https://doi.org/10.1007/s43440-020-00064-8

ARTICLE

Alpinumisoflavone suppresses hepatocellular carcinoma cell growth and metastasis via NLRP3 inflammasome-mediated pyroptosis

Yan Zhang[1] · Hong Yang[1] · Meifeng Sun[1] · Tingting He[1] · Yufang Liu[1] · Xiuwei Yang[1] · Xiaoli Shi[1] · Xiaoxiao Liu[1]

Received: 14 August 2019 / Revised: 15 December 2019 / Accepted: 13 February 2020 / Published online: 3 March 2020

Abstract

Aim This research aims to explore the effect of alpinumisoflavone (AIF) as an anti-cancer drug for the treatment of patients with hepatocellular carcinoma (HCC).

Methods Cell counting kit-8 (CCK-8) and colony formation assay were used to evaluate the viability of the cells and their clonogenic ability. Cellular migration and their invasion capabilities were detected using the wound-healing and transwell assay, respectively. The release of lactate dehydrogenase (LDH) was detected using the LDH kit. The expression levels of genes in the cells and tumor tissues were examined by qRT-PCR, western blotting, and immunohistochemical techniques. The cells transfected with mRFP-GFP-LC3 adenoviruses were stained to determine their autophagy status. MCC950 (NLRP3 inflammasome inhibitor) and NLRP3 shRNA were used to block NLRP3-mediated pyroptosis. Chloroquine and Atg 5 siRNA were used to inhibit the autophagy of the cells.

Results AIF suppressed cell proliferation, migration, and invasion capacity of SMMC 7721 and Huh7 cells. The incorporation of AIF induced the formation of NLRP3 inflammasome assembly, pyroptosis, and autophagy of the cells. However, the anti-proliferative and anti-metastatic effects of AIF on the HCC cells were attenuated by NLRP3 inhibitor and knockdown. Furthermore, Atg 5 knockdown inhibited autophagy and enhanced the rate of AIF-induced pyroptosis of the cells. AIF also suppressed tumor growth and increased the levels of pyroptosis-related genes in tumor tissues, which were consistent with in vitro observations.

Conclusion AIF inhibited HCC cell growth and metastasis by inducing NLRP3 inflammasome-mediated pyroptosis. Furthermore, AIF-induced autophagy augmented pyroptosis in HCC.

Keywords Alpinumisoflavone · Hepatocellular carcinoma · Pyroptosis · NLRP3 · Autophagy

Introduction

Liver cancer is the second most common cause of cancer-related deaths after lung cancer. According to the latest estimates, 841,080 new cases of liver cancer (4.7% of total cases) and 781,631 deaths due to liver cancer were reported in 2018 (8.2% of total cancer deaths) [1]. Hepatocellular carcinoma (HCC) is the most frequent type of liver cancer. Typically, molecular-targeted drugs and immunotherapy are used to treat patients having hepatitis B and hepatitis C virus, which cause HCC in humans. However, such patients at an early stage (50–80%) and advanced stages (20–44%) of liver cancer have a survival duration of 5 years [2]. The mortality rate does not improve with time, and hence the identification of novel strategies or therapeutic targets for the treatment of HCC is necessary.

Natural compounds and their derivatives play an irreplaceable role in the field of drug discovery due to their characteristics of high efficiency and low toxicity [3]. Most recently, bio-sourced derivatives such as saponins, flavonoids, alkaloids, and polyphenols were reported to be a promising candidate for anti-cancer activities. Numerous investigations were devoted to the screening of potential anti-tumor compounds from natural products, such as alpinumisoflavone (AIF), which is the principal bioactive

Electronic supplementary material The online version of this article (https://doi.org/10.1007/s43440-020-00064-8) contains supplementary material, which is available to authorized users.

✉ Xiaoxiao Liu
xxlqyf@126.com

[1] The Affiliated Hospital of Qingdao University, Jiangsu Road 16, Qingdao 266003, China

component of derriseriocarpa sourced from China that exhibits extensive pharmacological properties, such as molluscicidal [4], estrogenic [5], and antibacterial activities [6]. Recent studies have reported the anti-tumor activities of AIF in various malignancies, including clear cell renal cell carcinoma [7], esophageal squamous cell carcinoma (ESCC) [8], lung cancer [9], and colorectal cancer [10]. Besides, AIF serves as a potent radiosensitizer in ESCC. However, the effect of AIF on HCC cells and its underlying mechanisms has not been explored [11].

Pyroptosis is a form of caspase-1-dependent programmed cell death and is characterized by formation of membrane pores, fluid influx, plasma membrane rupture, leakage of cellular contents, cellular swelling, and lysis [12]. NLRP3 inflammasome is composed of NOD-like receptor family, pyrin domain-containing 3 (NLRP3), the adaptor ASC, and procaspase-1 [13]. Upon activation, NLRP3 recruits and cleaves procaspase-1 into its active forms (p20 and p10 subunit) which pre-process pro-IL-1β and pro-IL-18 into IL-1β and IL-18, respectively. Gasdermin D (GSDMD) performs the pyroptosis process, i.e., cleavage from the inflammatory caspase and IL-1β secretion. Inflammatory caspases cleave GSDMD into a 32-kDa N-terminal domain (GSDMD-N) and a 22-kDa C-terminal domain (GSDMD-C), respectively. The activation of pyroptosis promotes cell death and exerts anti-cancer effects on the cancerous cells. The deficiency of caspase-1 gene expression is reported to promote inflammation-induced colorectal cancer in mice [14, 15]. According to the latest literature, AIF can suppress tumor growth and metastasis by inducing apoptosis or autophagy; however, the co-relation between AIF and pyroptosis in HCC cells is still unknown.

In this manuscript, AIF suppressed cellular proliferation and metastasis by inducing pyroptosis via the activation of NLRP3 inflammasome. Also, the AIF-induced autophagy protected the HCC cells against pyroptosis.

Materials and methods

Materials

AIF (HPLC ≥ 98%, SMB00460) was obtained from Sigma-Aldrich (St. Louis, MO, USA) and dissolved in dimethylsulfoxide (DMSO, final concentration < 0.1%). Cell counting kit (CCK-8), LDH kit, Annexin V–FITC/PI apoptosis kit, and TUNEL kit were purchased from Beyotime Biotechnology (Shanghai, China). Primary antibodies against NLRP3, cleaved caspase-1, mature IL-1β, mature IL-18, GSDMD, and GSDMD-N, were obtained from Cell Signaling Technology (Danvers, MA, USA). Antibodies against p62, Atg 5, LC3B, and Beclin 1 were obtained from Abcam (Cambridge, MA, USA).

Cell lines and culture

Hepatocellular carcinoma cell lines (humans), HepG2, SMMC 7721, Huh7, Bel7402, healthy liver cells (humans), and LO2, were purchased from the cell banks of the Chinese Academy of Sciences (Shanghai, China). HepG2, SMMC 7721, Huh7, and Bel7402 cells were cultured in RPMI-1640 medium (Invitrogen Life Technologies, Carlsbad, CA, USA), while LO2 cell was maintained in the DMEM medium. The culture mediums were supplemented with 10% fetal bovine serum (Hyclone, Logan, UT, USA) and 1% penicillin/streptomycin. Cells were incubated in a humidified incubator at 37 °C, 5% CO_2.

Cell viability assessment

The CCK-8 assay was utilized to detect the effect of AIF on HCC cell proliferation by the manufacturer's protocol. In short, SMMC 7721 and Huh7 cells were seeded in 96-well plates (5×10^3 cells/well). After 24 h culture, the cells were exposed to different doses of AIF (0–20 μM) for the indicated duration. After the treatment, the medium was removed, and the cells were washed with 1 × PB, following which 10 μM CCK-8 was added to the cells and incubated at 37 °C for 1.5 h. The absorbance at 450 nm was examined using a spectrophotometer (Tecan Group Ltd., Männedorf, Switzerland).

Colony formation assay

SMMC 7721 and Huh7 cells in a logarithmic growth phase were plated in six-well plates (200 cells/well). Cells were then treated with different concentrations of AIF (0–20 μM) and incubated for 14 days. Then cells were fixed with 4% paraformaldehyde for 15 min and stained with 0.5% crystal violet, carefully rinsed with tap water, and dried at room temperature. The colonies with more than 50 cells were counted. Each result was obtained from three independently repeated experiments.

Wound healing assay

SMMC 7721 and Huh7 cells were cultured in a six-well plate to obtain 90% confluence, and a pipette tip was utilized to scratch a straight line on the cellular monolayer. First, the culture medium was removed, and the plates were washed three times with fresh medium. Then, cells were exposed to AIF (0–20 μM). After 48 h, the width of the open area was calculated, and the movement of the

cells was assessed by the degree of healing at the scratch surface.

Transwell assay

The 8-μm transwell filters (BD Biosciences, Franklin Lakes, NJ) were utilized to assess cell migration and invasion. In short, SMMC 7721 and Huh7 cells under different conditions were suspended in 0.5 mL serum-free media and added to the upper chamber with an uncoated or Matrigel-coated membrane. Moreover, the medium containing 10% FBS was added to the lower chamber. After 24 h culture, the cells that migrated and adhered to the bottom of the membrane were identified and colored differently. Five regions were randomly selected for each membrane. Each category of cells (migrating and invasive) was calculated and the average value was reported.

Lactate dehydrogenase (LDH) release assays

The effect of AIF on the release of lactate dehydrogenase (LDH) was detected by the LDH kit (Keygen Biotech, Nanjing, Jiangsu, China) following the manufacturer's protocols. Briefly, SMMC 7721and Huh7 cells were cultured in a 96-well plate and treated under different conditions. Next, the absorbance was assessed by using the microplate reader at 450 nm (Thermo Fisher Scientific, USA).

Qualitative polymerase chain reaction analysis

NLRP3, cleaved caspase-1, cleaved IL-1β, and IL-18 mRNA levels in SMMC 7721 and Huh7 cells were detected using qPCR. Total RNA in the cells were extracted using TRIzol reagent (Thermo Fisher Scientific, Waltham, MA). First-strand cDNA was synthesized using a reverse transcriptase kit (Applied Biosystems, Foster City, CA) following the manufacturer's protocols. qPCR was performed using the SYBR Green PCR Master Mix Kit (Applied Biosystems). The primer sequences used in the current study are listed in Table 1. GAPDH was regarded as an internal control. The mRNA levels were quantified using the $2^{-\Delta\Delta CT}$ method.

Acridine orange (AO) staining

The development of autophagic acidic vesicle organelles (AVO) was detected by acridine orange staining. Briefly, the cells were washed thrice with 1 × PBS, followed by treatment with AIF (0–20 μM) for 48 h. The red filter fluorescence microscope (BX53, OLYMPUS, Japan) was utilized to observe the cells which were dyed with 0.01% acridine orange (Solarbio, China) for 5 min.

Table 1 Primer sequences

Primer	Sequences (5′–3′)	Bases
F-NLRP3	GATCTTCGCTGCGATCAACAG	21
R-NLRP3	CGTGCATTATCTGAACCCCAC	21
F-caspase-1	CCTTAATATGCAAGACTCTCAAGGA	25
R-caspase-1	TAAGCTGGGTTGTCCTGCACT	21
F-IL-1β	ATGATGGCTTATTACAGTGGCAA	23
R-IL-1β	GTCGGAGATTCGTAGCTGGA	20
F-IL-18	TCTTCATTGACCAAGGAAATCGG	23
R-IL-18	TCCGGGGTGCATTATCTCTAC	21
F-GAPDH	ATCAC TGCCACCCAGAAGAC	20
R-GAPDH	TTTCTAGAC GGCAGGTCAGG	20

mRFP-GFP-LC3 adenovirus infection

SMMC 7721 and Huh7cells were transfected with mRFP-GFP-LC3 adenoviruses (Hanbio, Shanghai, China) for 48 h, followed by AIF (0–20 μM) for an indicated time. The effect of AIF on the formation of autophagosome and autolysosome was detected by imaging the cells at 400× magnification under a confocal microscope. Red spots and yellow spots represent autolysosome (mRFP) and autophagosome (RFP + GFP), respectively.

Animal experiment

Animal experiments were conducted following relevant guidelines and supported by the Medical Ethics Committee of the Affiliated Hospital of Qingdao University. In brief, the TPC-1 cells at a density of 1×10^6 were incubated into the back of nude mice to form PTC xenograft-bearing mice. When tumor volume reached approximately 100 mm^3, 18 tumor-bearing mice were randomly divided into three groups: vehicle control group, low-dose group (AIF: 20 mg/kg via gavage daily), and high-dose group (AIF: 40 mg/kg via gavage daily). Tumor volume and body weight of nude mice were measured and recorded every 3 days. Following 30 days of treatment, all nude mice were killed, and the final tumor volume was measured using a vernier caliper. The expression levels of NLRP3, caspase-1, cleaved IL-1β, and IL-18, and GSDMD-N in the tumor tissues were measured using the IHC assays.

Statistical analysis

The data were analyzed by SPSS 16.0 software package (SPSS Inc., Chicago, IL). One-way ANOVA and Dunnett's *t* test were used to compare cell lines, and p values < 0.05 were considered to be statistically significant.

Results

AIF treatment inhibited cell proliferation and clonogenic capacity in HCC cells

The chemical structure of AIF is shown in Fig. 1a. We investigated the cytotoxic effect of AIF on HepG2, SMMC 7721, Huh7, Bel7402, and healthy LO2 cells to understand its influence on HCC cells. The CCK-8 assay results confirmed the cytotoxic effect of AIF on HepG2, SMMC 7721, Huh7, and Bel7402 cell lines; however, it did not affect LO2 cellular growth but was selectively toxic to the HCC cells (Fig. 1b). Furthermore, the SMMC 7721 and Huh7 cells were sensitive to AIF (IC_{50} values: 39.3)

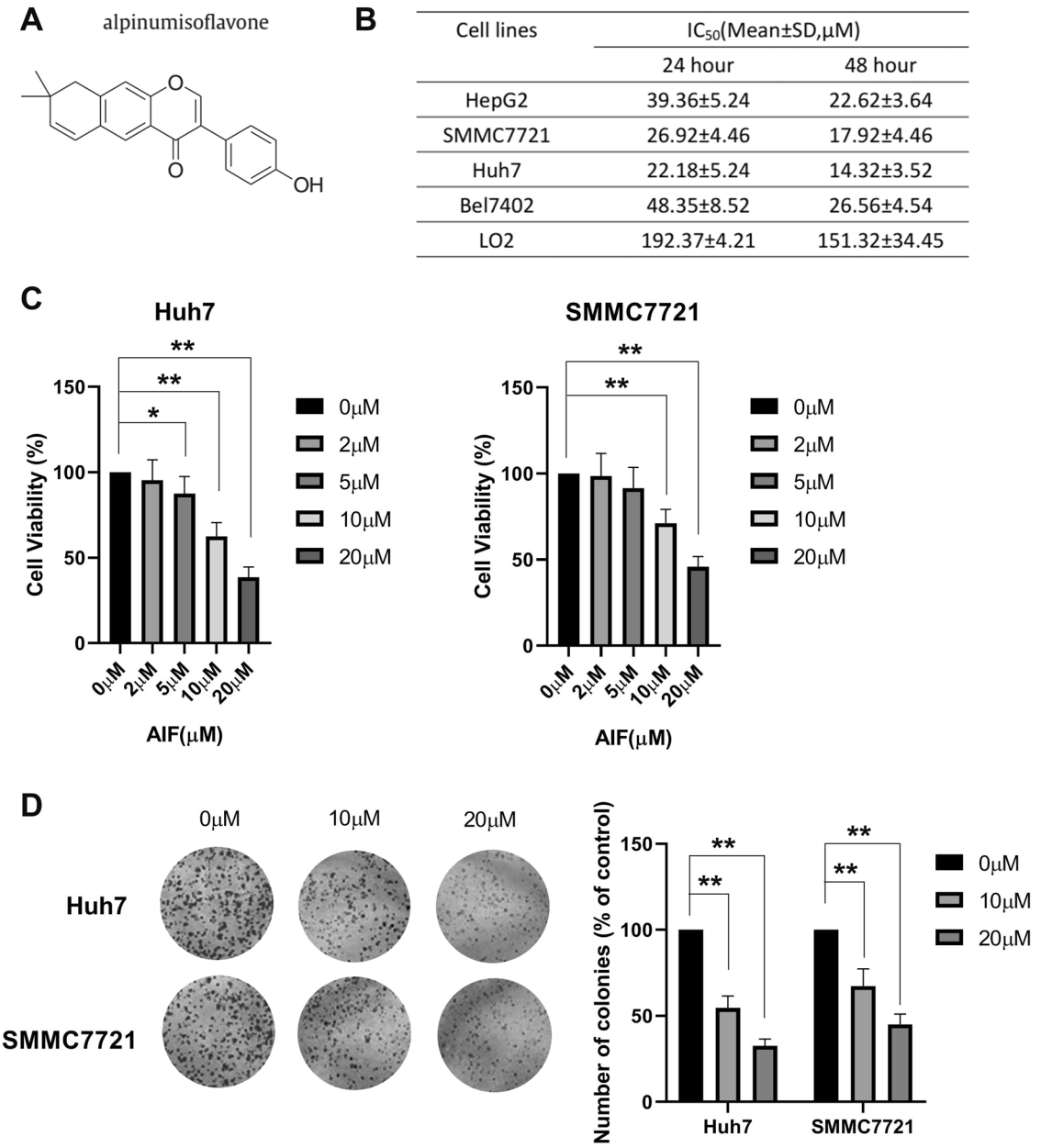

Cell lines	IC_{50}(Mean±SD,μM)	
	24 hour	48 hour
HepG2	39.36±5.24	22.62±3.64
SMMC7721	26.92±4.46	17.92±4.46
Huh7	22.18±5.24	14.32±3.52
Bel7402	48.35±8.52	26.56±4.54
LO2	192.37±4.21	151.32±34.45

Fig. 1 Effects of AIF on the HCC cell viability and clonogenic potential. **a** The chemical structure of alpinumisoflavone (AIF). **b** IC_{50} values of AIF in HepG2, SMMC 7721, Huh7, Bel7402, and LO2-treated cells were calculated after 24 h and 48 h, respectively. **c** Huh7 and Bel7402 cells were incubated with the varying dosage of AIF (0–20 μM) for 48 h, and the cell viability was evaluated using the CCK-8 assay. **d** Huh7 and Bel7402 cells were treated with AIF (0, 10, and 20 μM) for 14 days. Colony formation assay was employed to assess the colony generation ability. The data were presented as mean ± SD, and each result was obtained from at least three independent experiments (*$p < 0.05$, **$p < 0.01$)

(Fig. 1b, c) as compared to HepG2 and Bel7402 cells. Consequently, SMMC 7721 and Huh7 cells were chosen for further investigation, which verified the inhibitory effect of AIF on HCC cellular growth in the high-dose group (20 μM) (Fig. 1d), i.e., the number of colonies in AIF-treated cells was low as opposed to the control group.

AIF suppressed HCC cell migration and invasion capabilities

The anti-metastatic effect of AIF is related to human malignancies, and therefore we evaluated the effect of AIF treatment on the migration and invasion abilities of SMMC 7721 and Huh7 cell, respectively. As opposed to the control group, 10 and 20 μM of AIF dosage effectively reduced the migration of HCC cells ($p < 0.01$) (Fig. 2a). Also, the number of invasive cells in AIF-treated cells was markedly less than that in the control group ($p < 0.01$) (Fig. 2b). Furthermore, we also examined the influence of AIF on the protein expression level of matrix metalloproteinase-2 (MMP-2), matrix metalloproteinase-9 (MMP-9), and tissue inhibitor of metalloproteinases-3 (TIMP-3), which play a pivotal role in tumor cells metastasis. The western blotting analysis confirmed that AIF treatment down-regulated the level of MMP-2 and MMP-9, which increased the TIMP3 level in SMMC 7721 and Huh7 cells ($p < 0.01$) (Fig. 2c).

AIF induced NLRP3 inflammasome assembly and pyroptosis in SMMC 7721 and Huh7 cells

Pyroptosis is a class of caspase-1-dependent programmed cell death with anti-tumor effects. We detected the release of LDH, and levels of NLRP3, cleaved caspase-1, cleaved IL-1, cleaved IL-1β, and IL-18 to evaluate the effect of AIF on pyroptosis in SMMC 7721 and Huh7 cells. As shown in Fig. 3a, the rate of LDH release was significantly higher among AIF-treated cells than control ($p < 0.01$). Following AIF treatment, the mRNA (Fig. 3b), protein levels (Fig. 3c) of NLRP3, cleaved caspase-1, cleaved IL-1β, and IL-18 were notably elevated in SMMC 7721 and Huh7 cells in a dose-dependent manner ($p < 0.01$). These data suggested that AIF induced pyroptosis through NLRP3 -caspase-1-IL-1β and IL-18 pathways in the HCC cells.

Suppression of NLRP3 inflammasome attenuated the anti-proliferative and anti-metastatic effects of AIF in HCC cells

To further elucidate the co-relation between AIF-induced pyroptosis and NLRP3 inflammasome activation, MCC950, and NLRP3 inflammasome inhibitors were employed to block the formation of NLRP3 complex in SMMC 7721 and Huh7 cells. As shown in Fig. 4a, MCC950 had no noticeable impact on the protein expression levels of NLRP3, cleaved caspase-1, mature IL-1β, mature IL-18, GSDMD, and GSDMD-N in SMMC 7721 and Huh7 cells. MCC950 abolished the effect of AIF on the pyroptosis-related genes ($p < 0.01$) (Fig. 4a). AIF caused partial cell death of SMMC 7721 and Huh7 cells by inducing pyroptosis ($p < 0.01$) (Fig. 4b), whereas the HCC cells showed increased migratory and invasive capabilities ($p < 0.01$) (Fig. 4c, d). We inhibited pyroptosis in SMMC 7721 and Huh7 cells via the transfection of NLRP3 shRNA to confirm the anti-cancer effect of AIF in HCC cells. Figure 5a shows that NLRP3 levels were notably reduced in NLRP3 shRNA-transfected cells as compared to the control shRNA group ($p < 0.01$). Interestingly, no significant differences in cleaved caspase-1, mature IL-1β, mature IL-18, and GSDMD-N levels were observed among the control group and shRNA control group. In contrast, NLRP3 knockdown reduced the increase of cleaved caspase-1, mature IL-1β, mature IL-18, and GSDMD-N, which were mediated by AIF. Consequently, NLRP3 knockdown also attenuated the inhibitory effect of AIF on the viability (Fig. 5c) and motility (Fig. 5d, e) of SMMC 7721 and Huh7 cells. These observations signified that AIF-induced pyroptosis was dependent on NLRP3 inflammasome activation, and its effect on cell growth and motility was partially mediated by inducing pyroptosis.

AIF induced autophagy in HCC cells

We monitored the development of acidic vesicular organelles (AVOs) to investigate the effect of AIF on the autophagy of the SMMC 7721 and Huh7 cells. AIF promoted the formation of AVOs in a dose-dependent manner (Fig. 6a), i.e., an increase of red and green fluorescence (control) was observed in the cells with and without AIF treatment, respectively. We also studied the influence of AIF-induced autophagy of the cells after the transfection of the cells with mRFP-GFP-LC3 adenoviruses via the detection of autophagosome and autolysosome levels. Also, significant improvements were observed in autophagosome and autolysosome levels, as evident with the increase of yellow spots (RFP + GFP) and red spots (mRFP) (Fig. 6b). Typically, the conversion of cytosolic LC3-I to the autophagosome-associated LC3-II and p62 degradation are the two critical hallmarks of autophagy. Consequently, we examined the expressions of LC3BII/LC3BI, p62, and autophagy-related genes Beclin 1 and Atg 5 in the HCC cells. As presented in Fig. 6c, the dose-dependent exposure of AIF enhanced the conversion of LC3BII, and Beclin 1 to LC3BII and Atg 5, respectively; nevertheless, the expression of p62 declined ($p < 0.01$). These observations indicated that AIF treatment could enhance autophagy in the HCC cells.

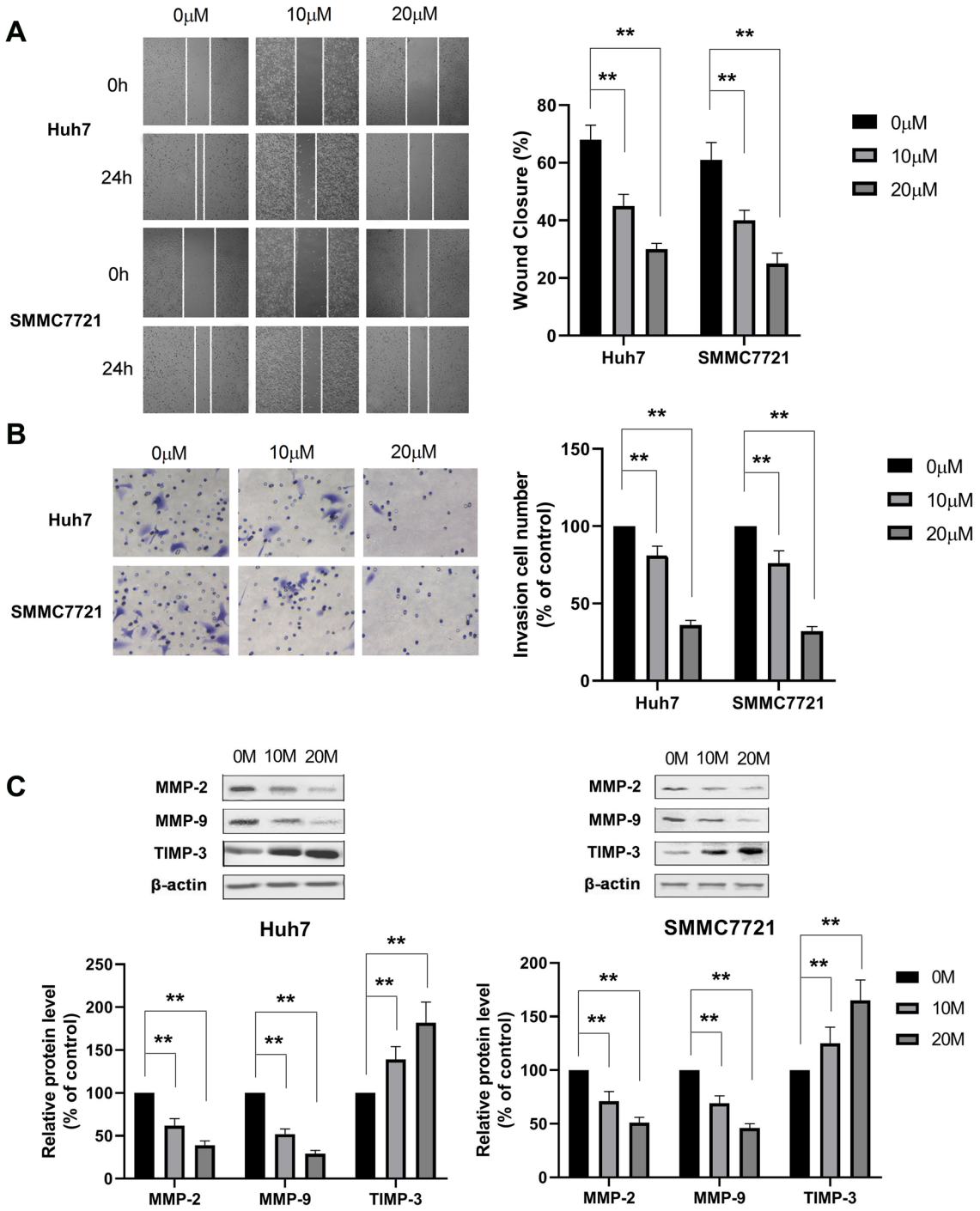

Fig. 2 Effects of AIF treatment on the HCC cell migration and invasion abilities. Huh7 and Bel7402 cells were treated with AIF (0, 10, and 20 μM) for 24 h. **a** Cell migration and **b** invasion capabilities were assessed by using wound healing assay and transwell assay. **c** The protein expression level of MMP-2, MMP-9, and TIMP-3 were analyzed by western blotting. The data were presented as mean ± SD, and each result was obtained from at least three independent experiments (*$p < 0.01$, **$p < 0.01$)

Inhibition of autophagy enhanced the AIF-induced pyroptosis in HCC cells

Recent studies have confirmed the complex interplay between autophagy and pyroptosis. Chloroquine (CQ), a specific autophagy inhibitor, was employed to block the autophagy process in cells in an attempt to study the effect of autophagy on AIF-induced pyroptosis in SMMC 7721 and Huh7 cells. As shown in Fig. 7a, CQ pretreatment significantly increased the release of LDH in AIF-treated

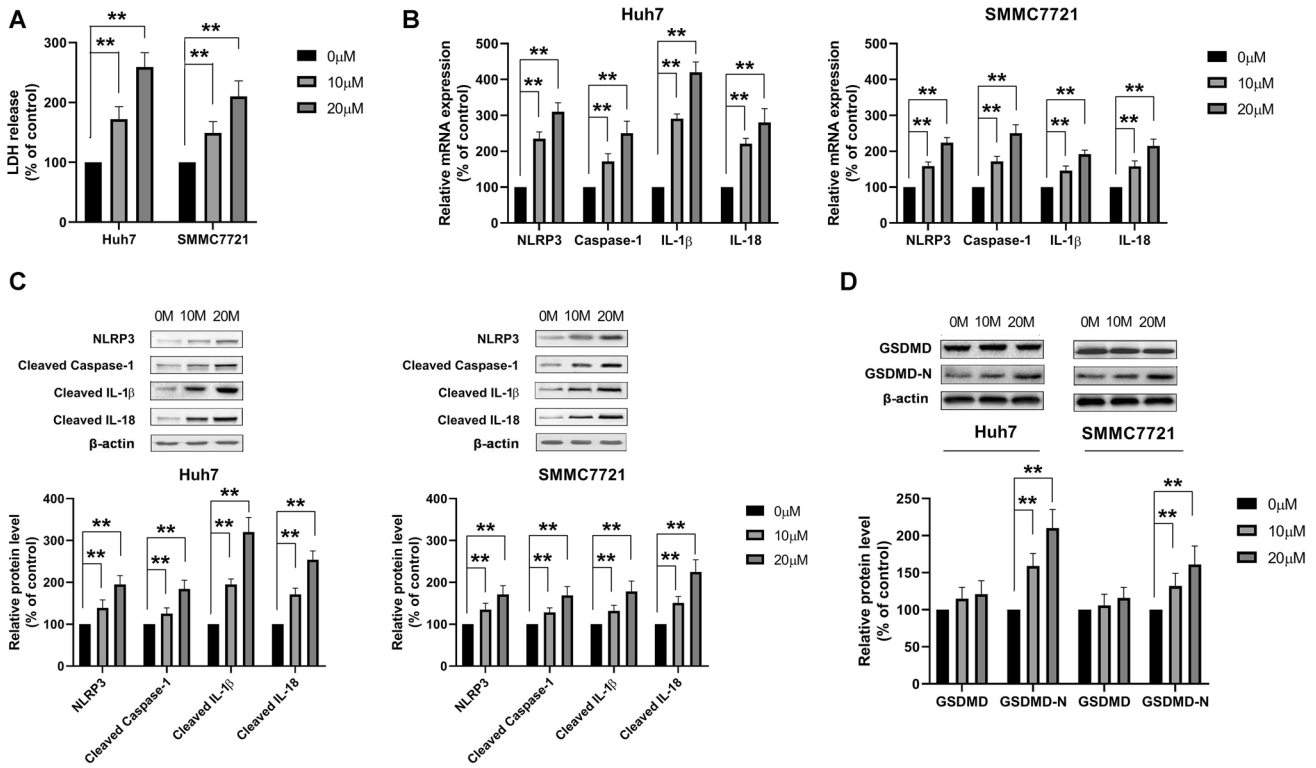

Fig. 3 AIF treatment induces pyroptosis in HCC cells. Huh7 and Bel7402 cells were incubated with AIF (0, 10, and 20 μM) for 48 h. **a** The release of LDH was evaluated by LDH Release Assay Kit. **b** mRNA and **c** protein expression levels of pyroptosis-related markers (NLRP3, cleaved caspase-1, cleaved IL-1β, and IL-18) were evaluated by qRT-PCR and western blotting, respectively. **d** The cleavage of GSDMD was analyzed by western blotting. β-actin was chosen as an internal control. GSDMD: gasdermin D, GSDMD-N: gasdermin D N-domain. The data were presented as mean ± SD, and each result was obtained from at least three independent experiments (*$p < 0.05$, **$p < 0.01$)

cells ($p < 0.05$). Besides, CQ co-treatment also enhanced the AIF-induced increase of NLRP3, cleaved caspase-1, mature IL-1β, IL-18, and GSDMD-N in SMMC 7721 and Huh7 cells ($p < 0.01$) (Fig. 7b). The relationship between autophagy and pyroptosis was verified by the transfecting of the HCC cells with targeted Atg 5 siRNA or control siRNA, which were exposed to AIF (20 μM). As observed, the silencing Atg 5 enhanced the amount of LDH release ($p < 0.05$) (Fig. 7c) as well as the level of NLRP3, cleaved caspase-1, mature IL-1β, IL-18, and GSDMD-N ($p < 0.01$) (Fig. 7d) in the AIF-treated cells. These results suggested that autophagy could regulate AIF-induced pyroptosis in HCC cells via a self-protective mechanism.

AIF suppressed tumor growth and induced NLRP3-dependent pyroptosis in a xenograft mouse model

Next, we then verified the in vitro observations in the HCC xenograft mouse model. As observed, AIF treatment effectively reduced the tumor volume and weight in a dose-dependent manner in comparison to a vehicle group ($p < 0.01$) (Fig. 8a, b). However, no significant difference in body weight (Fig. 8c) and histopathological changes of heart, liver, spleen, lung, and kidney (Supplementary Fig. 1) were observed among the treated and untreated groups, respectively. Besides, immunohistochemical results showed that AIF could elevate the expression levels of NLRP3, cleaved caspase-1, mature IL-1β, IL-18, and GSDMD-N in tumor tissues as compared to the control group (Fig. 8d). Likewise, in vivo experiments verified that pyroptosis was involved in the anti-growth effect of AIF in HCC cells.

Discussion

Natural products/herbal medicines have anti-cancer properties, and therefore can be used either standalone or in combination with conventional chemotherapeutic agents in a clinical setting [16, 17]. The anti-cancer properties of flavonoids, a significant component in several medicinal plants, have been extensively studied in a variety of malignancies that occur in humans. In 2001, the cytotoxic activities of AIF as an active ingredient was first

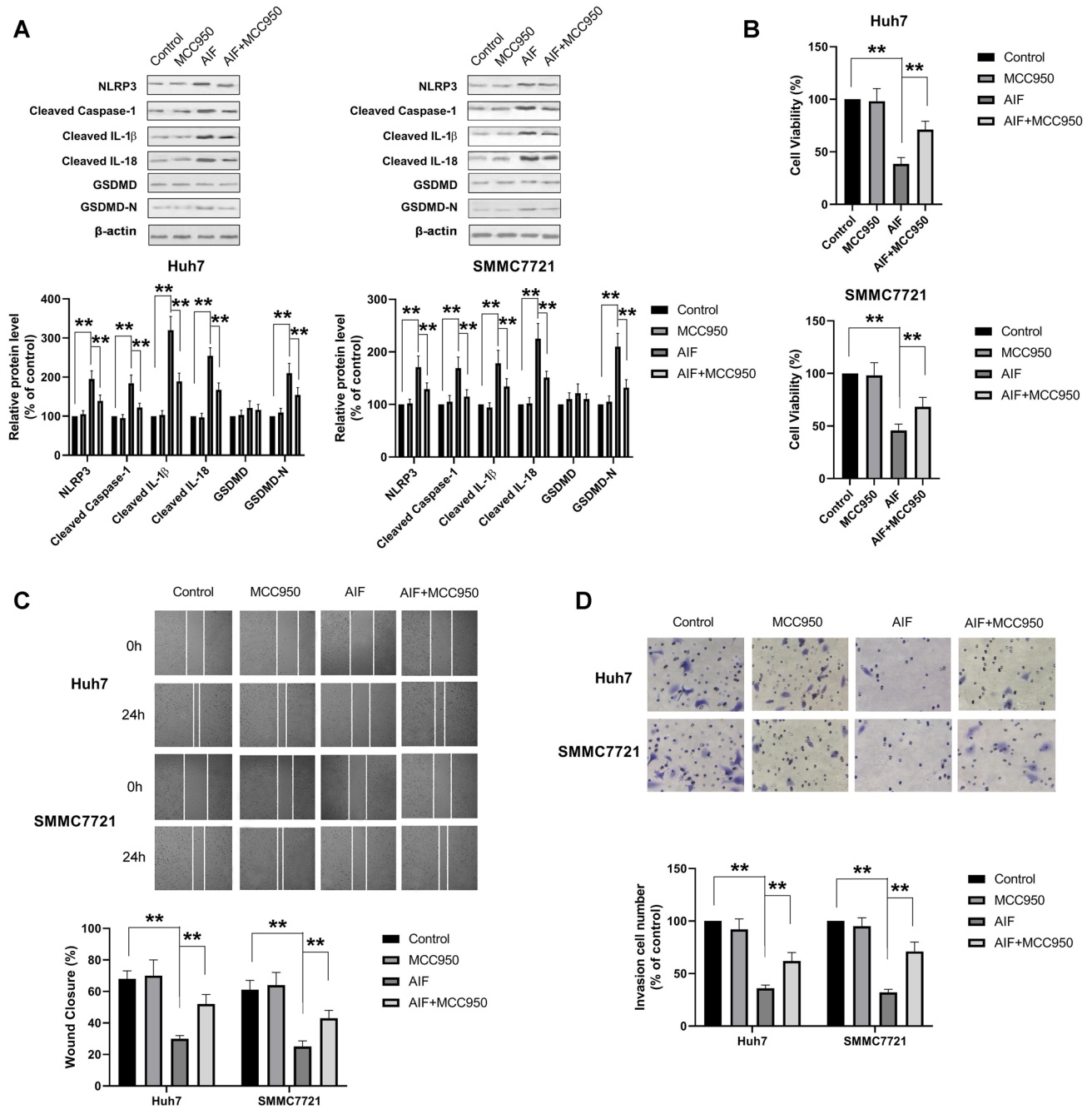

Fig. 4 Inflammasome inhibition reverses the anti-proliferative and anti-metastatic effects of AIF in HCC cells. Huh7 and Bel7402 cells were treated with 20 μM AIF in the presence or absence of NLRP3 inflammasome inhibitor MCC950. **a** Protein levels of NLRP3, cleaved caspase-1, mature IL-1β, mature IL-18, GSDMD, and GSDMD-N in cells as detected by western blotting. β-actin was chosen as an internal control. **b** Cell viability was assessed by CCK-8 assay. **c** Cell migration and **d** invasion ability were evaluated by wound healing assay and Transwell assay. The data were presented as mean ± SD, and each result was obtained from at least three independent experiments (*$p < 0.05$, **$p < 0.01$)

reported in vitro in nasopharyngeal carcinoma cells [18]. AIF can promote apoptotic cell death via repressing both the extracellular signal-regulated kinases/mitogen-activated protein kinase (ERK/MAPK) and nuclear factor-κB (NF-κB) pathways [9]. Moreover, the anti-leukemic activities of AIF can inhibit STAT signaling [19]. MiR-370 has been identified as the molecular target responsible for the pro-apoptotic activities in esophageal squamous cell

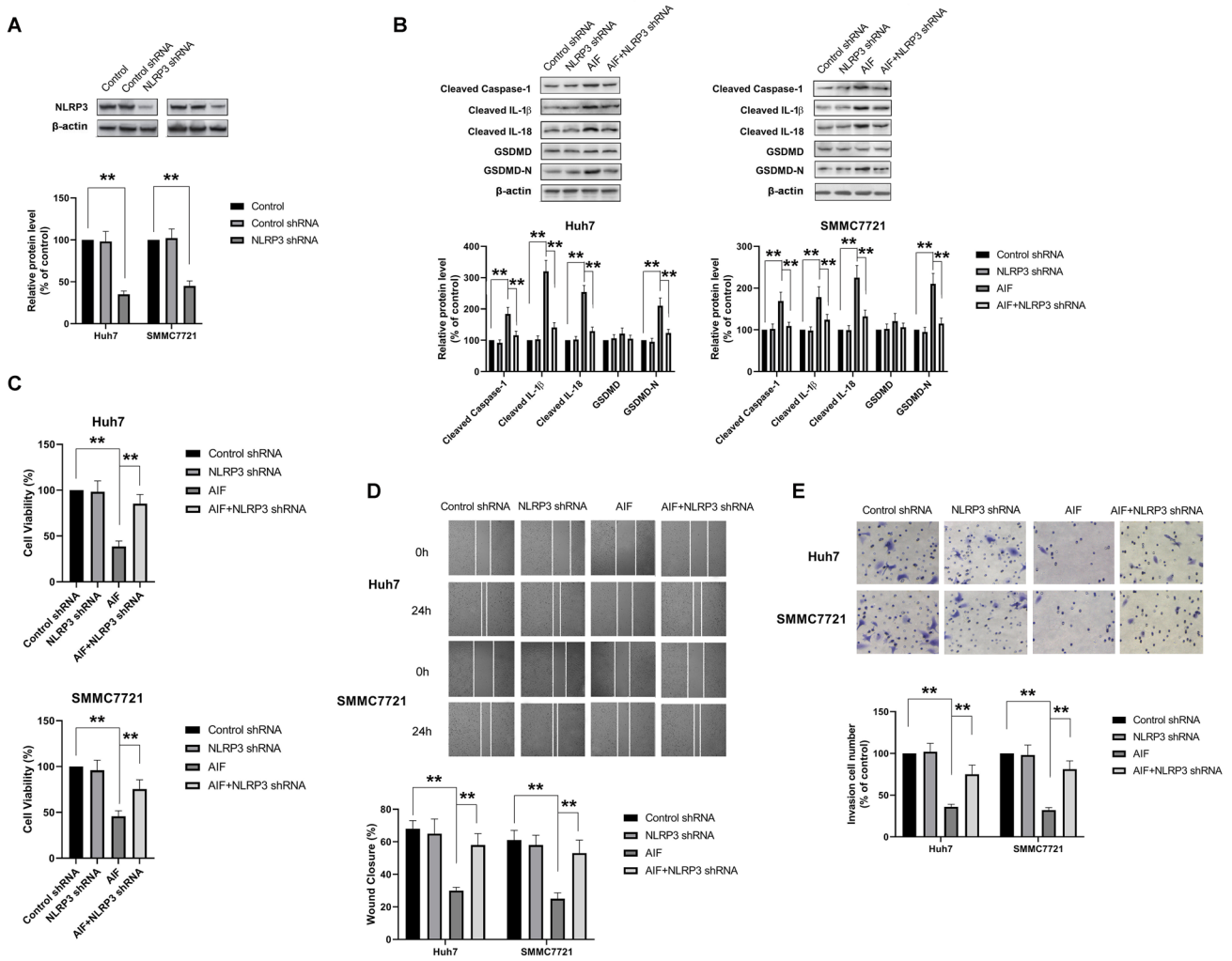

Fig. 5 NLRP3 knockdown alleviates the inhibitory effect of AIF on HCC cell viability, migration, and invasion**. a** Following transfection of Huh7 and Bel7402 cells with NLRP3 shRNA or control shRNA for 48 h, the protein expression of NLRP3 was confirmed by western blotting. β-actin was chosen as an internal control. Cells transfected with NLRP3 shRNA with, and without 20 μM AIF were incubated for 48 h. **b** Protein levels of NLRP3, cleaved caspase-1, mature IL-1β, mature IL-18, GSDMD, and GSDMD-N in Huh7 and Bel7402 cells were examined by western blotting. β-actin was chosen as an internal control. **c** Cell viability was assessed by CCK-8 assay. **d** Cell migration and **e** invasion ability were evaluated by wound healing assay and transwell assay. The data were presented as mean ± SD, and each result was obtained from at least three independent experiments (*$p < 0.05$, **$p < 0.01$)

carcinoma [8]. Besides, miR-101 is also reported to be the primary target for the anti-growth and anti-metastatic activities of AIF against clear cell renal carcinoma [7]. The anti-metastatic activities of AIF against melanoma cells were reported to be associated with the downregulation of COX-2 via the modulation of the miR-124/SPHK1 axis [20]. The ability of AIF to block cell cycle progression is observed in esophageal squamous cell carcinoma [11]. In colorectal cancer, AIF is reported to suppress tumor growth and metastasis by blocking RAD51-mediated DNA repair [10]. In the present study, the role of AIF in HCC is explored. Our findings revealed that AIF could exhibit anti-growth activities and suppress the metastatic potential of HCC cell by triggering NLRP3 inflammasome-mediated pyroptosis. Moreover, our results showed that AIF-induced autophagy could protect HCC cells against the pro-pyroptotic activities of AIF. Pyroptosis is reported to cause anti-cancer activities of most chemotherapeutic agents, such as 5-FU, which is a newly identified form of programmed cell death (PCD) [21]. In the context of HCC, the activation of pyroptosis adds extra benefits [22, 23]. Pyroptosis can occur via canonical and

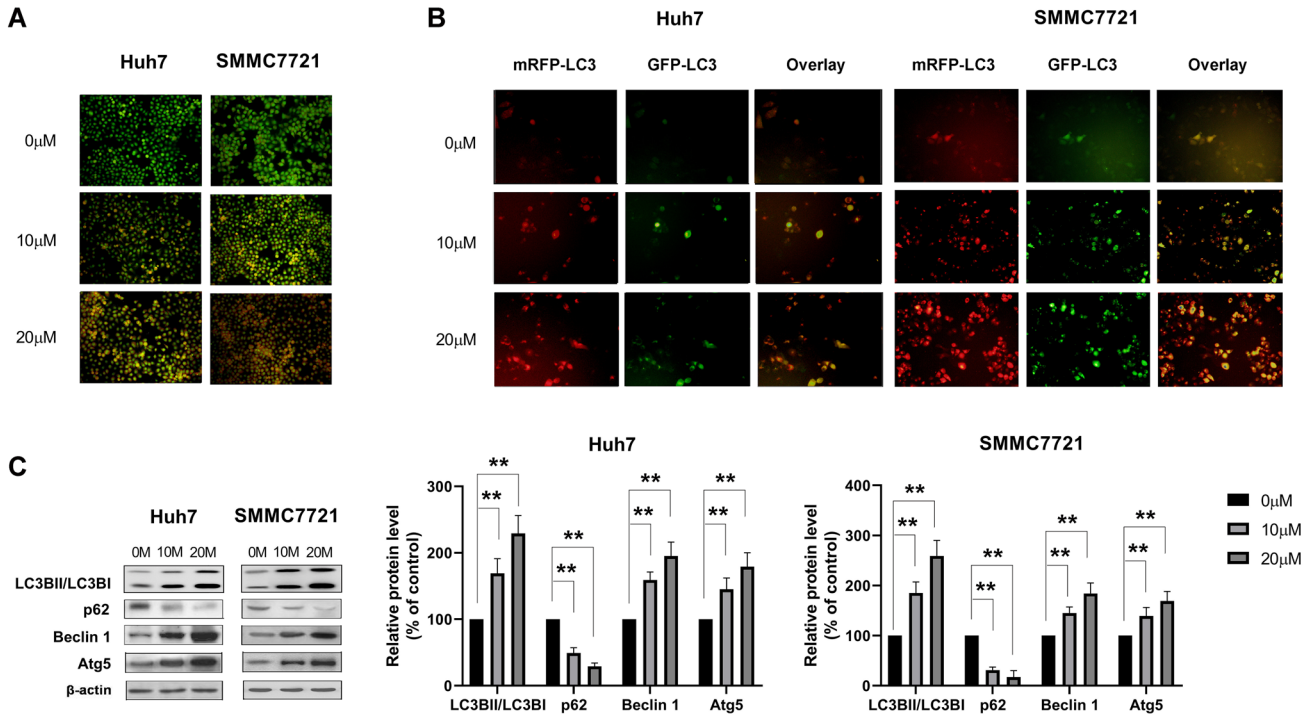

Fig. 6 AIF induces autophagy in HCC cells**.** Huh7 and Bel7402 cells were incubated for 48 h with 0, 10, and 20 μM AIF. **a** The formation of acidic vesicle organelles (AVO) in AIF-treated cells was observed and photographed under a fluorescence microscope (magnification: 200×) following acridine orange staining. **b** Huh7 and Bel7402 cells were transfected with mRFP-GFP-LC3 adenoviruses for 48 h. The effect of AIF on the formation of autophagosome and autolysosome was observed under a fluorescence microscope (magnification: 400×). Red spots (mRFP): autolysosome; Yellow spots: autophagosome (RFP + GFP). **c** The protein levels of autophagy-related markers, LC3B, p62, Beclin 1, and Atg 5 in Huh7 and Bel7402 cells as detected by western blotting. β-actin was chosen as an internal control. The data were presented as mean ± SD, and each result was obtained from at least three independent experiments (**$p < 0.01$)

non-canonical pathways, depending on the activation of caspase-1 and caspase-11(caspase-4/5 in humans). In the canonical pathway, the formation of inflammasomes activates caspase-1, which subsequently cleaves GSDMD to form the N-terminal fragment. The N domain of GSDMD translocates to the cell membrane that promotes perforation [22]. Among all inflammasomes, NLRP3, including NLRP3, ASC, and caspase-1, has been widely examined. The activation of NLRP3 inflammasome promotes cleavage of caspase-1, which processes pro-IL-18 and pro-1β to their mature forms [13]. In our results, we found that AIF could activate the NLRP3 inflammasome in a dose-dependent fashion, as demonstrated by the elevated expression level of NLRP3 and cleaved caspase-1. Besides, AIF treatment caused the cleavage of IL-18 and IL-1β as well as an increased level of GSDMD-N, which confirmed the pyroptosis-induced effect of AIF in HCC cells. Furthermore, the shRNA markedly abolished the anti-cancer activities of AIF against HCC cells after the pyroptosis induction was blocked by inhibitor or NLRP3. These results provided experimental evidence that AIF could show anti-cancer activities on HCC that triggers pyroptosis. Autophagy is a multi-step process that includes the formation of autophagosomes with sequestered cellular components, fusion with lysosomes, and degradation of autophagic cargoes in autophagolysosome [24, 25]. Although autophagy results in cell death, studies show that autophagy also plays a pro-survival role in cells [26]. Yu et al. [26] showed that inhibition of eukaryotic elongation factor-2 kinase-induced autophagy enhanced pyroptosis in doxorubicin-treated human melanoma cells in vitro. The pro-pyroptotic activities of E2 were augmented by inhibition of autophagy with 3-MA in HCC cells [22]. In line with these previous findings, our results showed that blockage of AIF-induced autophagy in HCC cells by CQ or Atg5 siRNA could augment its pro-pyroptotic activities against HCC cells. These combined results showed that autophagy could be a negative regulatory factor against AIF-induced pyroptosis in HCC cells.

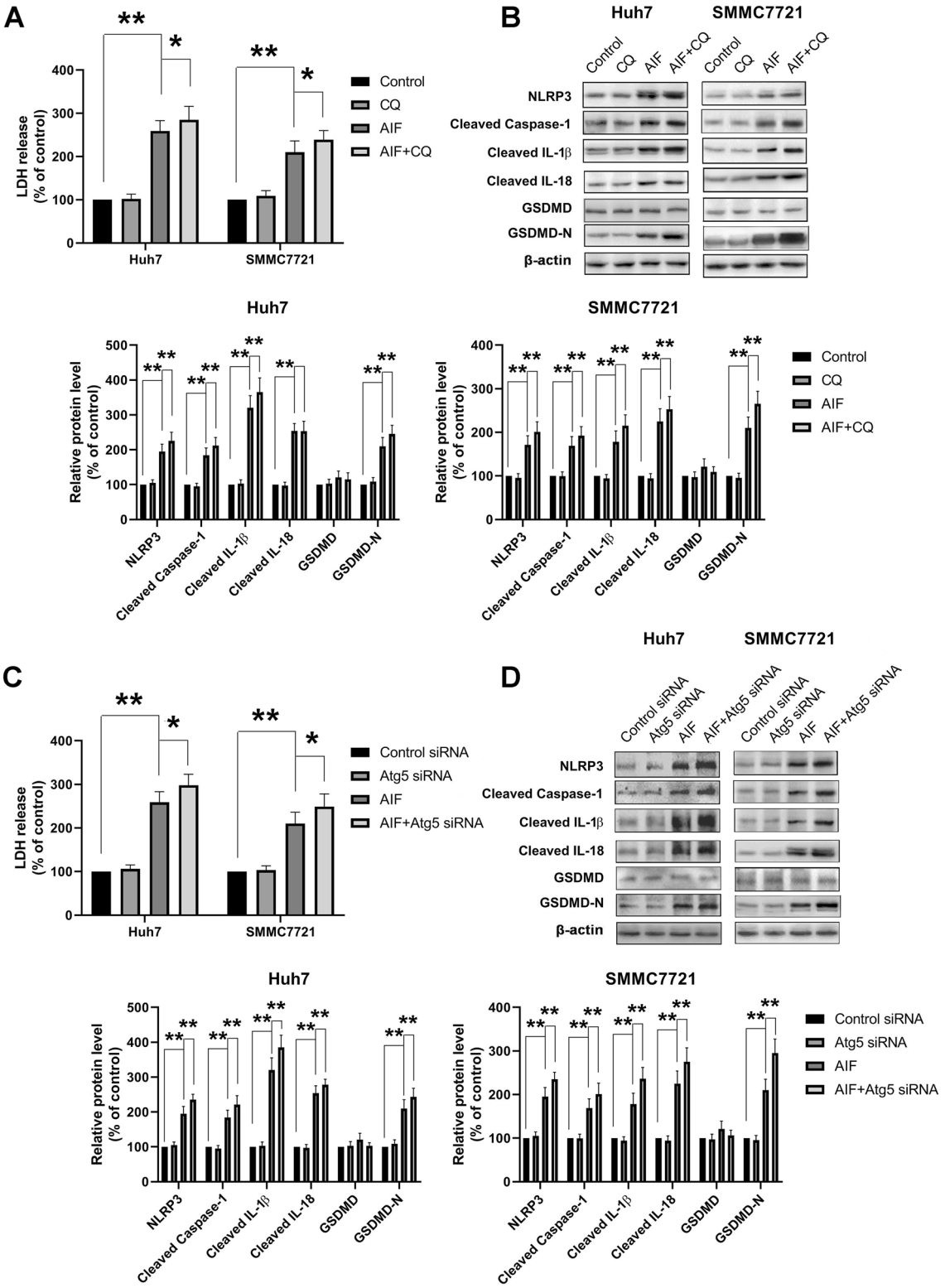

Fig. 7 Blocking autophagy abolishes AIF-induced pyroptosis in HCC cells. Huh7and Bel7402 cells were transfected with or without Atg 5 siRNA or control siRNA, then treated with 20 μM AIF or 20 μM AIF + CQ (autophagy inhibitor) for 48 h. **a**, **c** LDH Release Assay Kit was used to evaluate the release of LDH. **b**, **d** The protein levels of autophagy-related markers, LC3B, p62, Beclin 1, and Atg 5 in Huh7 and Bel7402 cells as detected by western blotting. β-actin was chosen as an internal control. The data were presented as mean ± SD, and each result was obtained from at least three independent experiments (**$p < 0.01$)

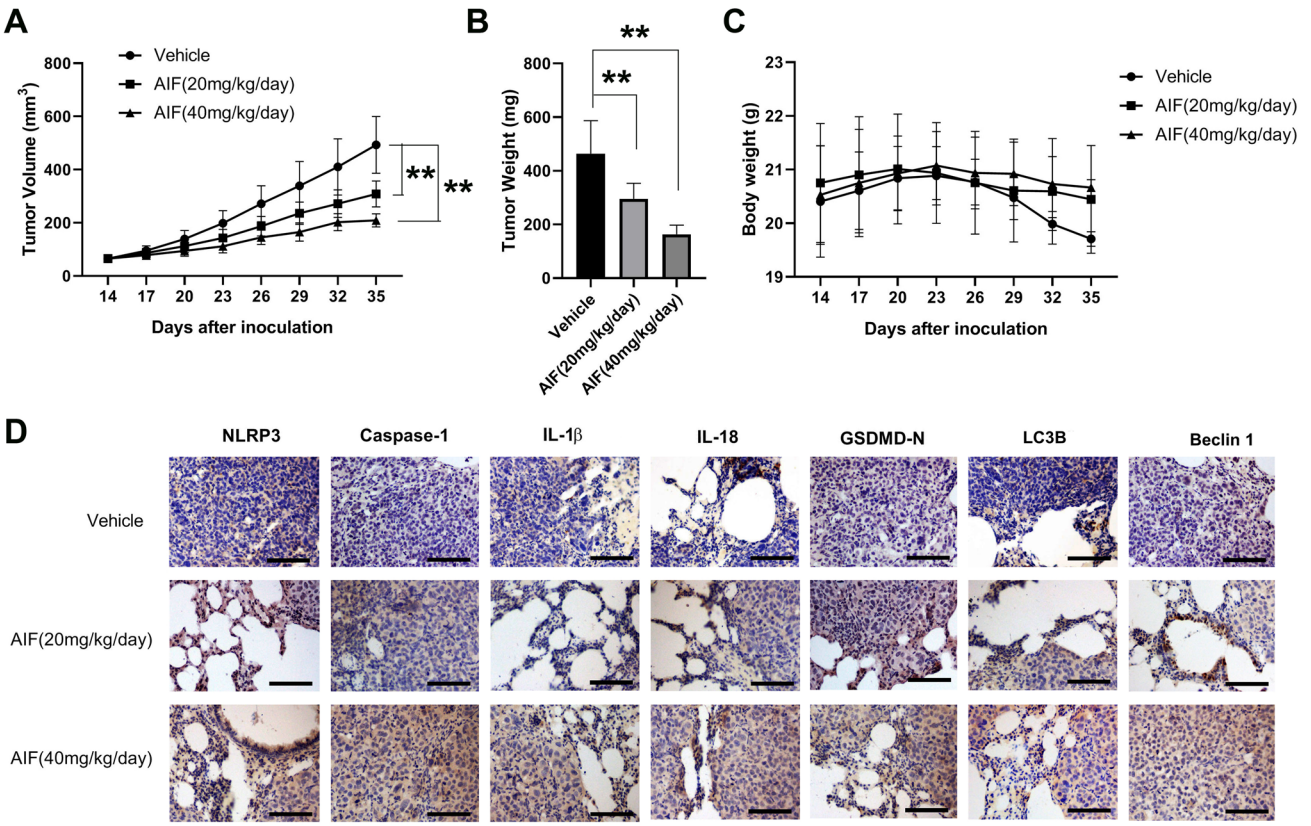

Fig. 8 AIF suppresses tumor growth in HCC xenograft model. HCC-bearing mice were treated with vehicle or AIF (20, and 40 mg/kg/daily) for 21 days (tumor volume: 100 mm^3). **a** Tumor volume and **c** body weight were calculated and recorded every 3 days. **b** Tumor weight was recorded after removing from mice. **d** The abundance of NLRP3, caspase-1, cleaved IL-1β, and IL-18, and GSDMD-N in tumor tissues was evaluated by immunohistochemistry. Data were presented as mean ± SD, and each result was obtained from at least three independent experiments (**$p < 0.01$)

Conclusion

In the present study, the anti-cancer effect of AIF on HCC cells and its underlying mechanisms were explored. Our data revealed that AIF could suppress cell proliferation and metastasis by inducing pyroptosis-mediated activation of the NLRP3 inflammasome. Moreover, autophagy induced by AIF performed a protective role against pyroptosis in HCC cells.

Author contributions XL designed the research and wrote the paper. YZ, HY, MS, and TH performed the experiments. YL, XY, and XS analyzed the data and collected the information.

Funding None.

Compliance with ethical standards

Conflict of interest The author(s) declare that they have no conflict of interests.

References

1. Bray F, Ferlay J, Soerjomataram I, Siegel RL, Torre LA, Jemal A. Global cancer statistics 2018: GLOBOCAN estimates of incidence and mortality worldwide for 36 cancers in 185 countries. CA Cancer J Clin. 2018;68:394–424.
2. Llovet JM, Villanueva A, Lachenmayer A, Finn RS. Advances in targeted therapies for hepatocellular carcinoma in the genomic era. Nature Rev Clin Oncol. 2015;12:408–24.
3. Ahmed F, Ishibashi M. Bio-active natural products with TRAIL-resistance overcoming activity. Chem Pharm Bull. 2016;64:119–27.
4. Lyddiard JR, Whitfield PJ. Inhibition of site I mitochondrial electron transport by an extract of the seeds of *Millettia thonningii*: a potential mechanism for the plant's molluscicidal and schistosome larvicidal activity. J Helminthol. 2001;75:259–65.
5. Mvondo MA, Njamen D, Tanee Fomum S, Wandji J. Effects of alpinumisoflavone and abyssinone V-4'-methyl ether derived from *Erythrina lysistemon* (Fabaceae) on the genital tract of

ovariectomized female Wistar rat. Phytotherapy Res PTR. 2012;26:1029–36.
6. Chukwujekwu JC, Van Heerden FR, Van Staden J. Antibacterial activity of flavonoids from the stem bark of *Erythrina caffra* thunb. Phytother Res. 2011;25:46–8.
7. Wang T, Jiang Y, Chu L, Wu T, You J. Alpinumisoflavone suppresses tumour growth and metastasis of clear-cell renal cell carcinoma. Am J Cancer Res. 2017;7:999–1015.
8. Han Y, Yang X, Zhao N, Peng J, Gao H, Qiu X. Alpinumisoflavone induces apoptosis in esophageal squamous cell carcinoma by modulating miR-370/PIM1 signaling. Am J Cancer Res. 2016;6:2755–71.
9. Namkoong S, Kim TJ, Jang IS, Kang KW, Oh WK, Park J. Alpinumisoflavone induces apoptosis and suppresses extracellular signal-regulated kinases/mitogen activated protein kinase and nuclear factor-kappaB pathways in lung tumor cells. Biol Pharm Bull. 2011;34:203–8.
10. Li D, Li X, Li G, Meng Y, Jin Y, Shang S, et al. Alpinumisoflavone causes DNA damage in colorectal cancer cells via blocking DNA repair mediated by RAD51. Life Sci. 2019;216:259–70.
11. Zhang B, Fan X, Wang Z, Zhu W, Li J. Alpinumisoflavone radiosensitizes esophageal squamous cell carcinoma through inducing apoptosis and cell cycle arrest. Biomed Pharmacotherapy. 2017;95:199–206.
12. Bergsbaken T, Fink SL, Cookson BT. Pyroptosis: host cell death and inflammation. Nature Rev Microbiol. 2009;7:99–109.
13. Franchi L, Munoz-Planillo R, Nunez G. Sensing and reacting to microbes through the inflammasomes. Nature Immunol. 2012;13:325–32.
14. Ummanni R, Lehnigk U, Zimmermann U, Woenckhaus C, Walther R, Giebel J. Immunohistochemical expression of caspase-1 and -9, uncleaved caspase-3 and -6, cleaved caspase-3 and -6 as well as Bcl-2 in benign epithelium and cancer of the prostate. Exp Therapeutic Med. 2010;1:47–52.
15. Winter RN, Kramer A, Borkowski A, Kyprianou N. Loss of caspase-1 and caspase-3 protein expression in human prostate cancer. Cancer Res. 2001;61:1227–322.
16. Yue Q, Gao G, Zou G, Yu H, Zheng X. Natural products as adjunctive treatment for pancreatic cancer: recent trends and advancements. BioMed Res Int. 2017;2017:8412508.
17. Yuan R, Hou Y, Sun W, Yu J, Liu X, Niu Y, et al. Natural products to prevent drug resistance in cancer chemotherapy: a review. Ann N Y Acad Sci. 2017;1401:19–27.
18. Nkengfack AE, Azebaze AG, Waffo AK, Fomum ZT, Meyer M, van Heerden FR. Cytotoxic isoflavones from *Erythrina indica*. Phytochemistry. 2001;58:1113–20.
19. Kumar S, Pathania AS, Saxena AK, Vishwakarma RA, Ali A, Bhushan S. The anticancer potential of flavonoids isolated from the stem bark of *Erythrina suberosa* through induction of apoptosis and inhibition of STAT signaling pathway in human leukemia HL-60 cells. Chem Biol Interact. 2013;205:128–37.
20. Gao M, Chang Y, Wang X, Ban C, Zhang F. Reduction of COX-2 through modulating miR-124/SPHK1 axis contributes to the anti-metastatic effect of alpinumisoflavone in melanoma. Am J Transl Res. 2017;9:986–98.
21. Wang Y, Yin B, Li D, Wang G, Han X, Sun X. GSDME mediates caspase-3-dependent pyroptosis in gastric cancer. Biochem Biophys Res Commun. 2018;495:1418–25.
22. Wei Q, Zhu R, Zhu J, Zhao R, Li M. E2-induced activation of the NLRP3 inflammasome triggers pyroptosis and inhibits autophagy in HCC cells. Oncol Res. 2019;27:827–34.
23. Han M, Gao H, Xie J, Yuan YP, Yuan Q, Gao MQ, et al. Hispidulin induces ER stress-mediated apoptosis in human hepatocellular carcinoma cells in vitro and in vivo by activating AMPK signaling pathway. Acta Pharmacol Sin. 2019;40:666–76.
24. Yoshii SR, Mizushima N. Monitoring and measuring autophagy. Int J Mol Sci. 2017;2017:18.
25. Han M, Gao H, Ju P, Gao MQ, Yuan YP, Chen XH, et al. Hispidulin inhibits hepatocellular carcinoma growth and metastasis through AMPK and ERK signaling mediated activation of PPAR-gamma. Biomed Pharmacotherapy. 2018;103:272–83.
26. Yu P, Wang HY, Tian M, Li AX, Chen XS, Wang XL, et al. Eukaryotic elongation factor-2 kinase regulates the cross-talk between autophagy and pyroptosis in doxorubicin-treated human melanoma cells in vitro. Acta Pharmacol Sin. 2019;40:123–1244.